frontiers in Materials

ORIGINAL RESEARCH
published: 13 August 2021
doi: 10.3389/fmats.2021.733257

The Effect of Pyrolysis Conditions on the Preparation of Fe_2O_3 Particles Using Simulated Pickling Liquor in a Venturi Reactor

Chao Lv[1,2]*, *Ming-He Sun*[1] and *Hong-Xin Yin*[1]

[1]School of Control Engineering, Northeastern University, Qinhuangdao, China, [2]Key Laboratory for Ferrous Metallurgy and Resources Utilization of Ministry of Education, Wuhan University of Science and Technology, Wuhan, China

Large amounts of pickling liquor are produced during the pickling of iron and steel. The Venturi reactor is used during the pyrolysis of pickling liquor to prepare high-purity Fe_2O_3 particles. Changing the pyrolysis conditions will affect the purity and concentration of Fe_2O_3 particles. In this paper, physical experiments and numerical simulations were carried out to study the effect of pyrolysis conditions on the Fe_2O_3 particles, including the pyrolysis temperature, the $FeCl_2$/$FeCl_3$ ratio in the pickling liquor, and the citric acid ratio. The results showed that a product with a higher purity, better crystallinity, and greater concentration was obtained at 923 K. Further increasing the temperature did not change the concentration of Fe_2O_3 particles. When the ratio of $FeCl_2$/$FeCl_3$ in the pickling liquor was 1:1.5, the maximum concentration of Fe_2O_3 particles at the outlet was obtained. When the added proportion of citric acid was 1:1, the particle size distribution was more uniform, and when the added proportion was 1:2.5, the maximum concentration of Fe_2O_3 particles at the outlet was achieved.

Keywords: pickling liquor, pyrolysis, Fe_2O_3, particles, numerical simulation

OPEN ACCESS

Edited by:
Wangzhong Mu,
Royal Institute of Technology, Sweden

Reviewed by:
Yuming Wen,
Royal Institute of Technology, Sweden
Fengqin Liu,
University of Science and Technology Beijing, China
Zongliang Zhang,
Central South University, China

***Correspondence:**
Chao Lv
lvchao@neuq.edu.cn

Specialty section:
This article was submitted to Colloidal Materials and Interfaces, a section of the journal Frontiers in Materials

Received: *30 June 2021*
Accepted: *03 August 2021*
Published: *13 August 2021*

Citation:
Lv C, Sun M-H and Yin H-X (2021) The Effect of Pyrolysis Conditions on the Preparation of Fe_2O_3 Particles Using Simulated Pickling Liquor in a Venturi Reactor. Front. Mater. 8:733257. doi: 10.3389/fmats.2021.733257

INTRODUCTION

The dense Fe_2O_3 formed on the surface of steel products during their production requires pickling, which produces 1.2–2 tons of pickling liquor per ton of steel (Zhang et al., 2014; Wang and Ma, 2017; Wang et al., 2020). HCl pickling liquor contains 1–5% HCl and 5–20% $FeCl_2$/$FeCl_3$, which causes severe environmental issues if discharged directly, as well as resource waste (Fang et al., 2010; Gao et al., 2021). In large iron and steel enterprises, the Ruthner spray pyrolysis method (Qi, 2006; Deng et al., 2007; Bian et al., 2015) is primarily used to process waste acid, in which $FeCl_2$ and $FeCl_3$ react with H_2O and O_2 to produce HCl and Fe_2O_3 particles. Nevertheless, this process has technical barriers and high investment costs. To decrease costs and increase the value of by-products, an in-depth study of the pyrolysis technique is needed. Sun et al. (2021) prepared the nanometer ferric oxide (Fe_2O_3 nanorod) by the hydrothermal method, the ferric nitrate nonahydrate ($Fe(NO_3)_3{\cdot}9H_2O$) was the source of ferric and the ethanol absolute and ethylenediamine were used as the surfactant. Effects of the reaction temperature and the mass fraction of $Fe(NO_3)_3{\cdot}9H_2O$ on the particle size of the Fe_2O_3 nanorod were investigated. Zhang et al. (2020) prepared the α-nanometer Fe_2O_3 by microwave hydrolysis, $FeCl_3$ was the raw material and the triethylenetetramine (TETA) was used as the coordination agent. Taniguchi (Izumi et al., 2007) synthesized $LiMn_2O_4$ particles with a hollow sphere morphology from a precursor solution using spray pyrolysis from a slurry solution and prepared spherical $LiMn_2O_4$ nanoparticles. Liu et al. (2018) designed a spray pyrolysis reactor using SiC and prepared MgO with an average particle size of 90 μm. They also studied parameters such as the

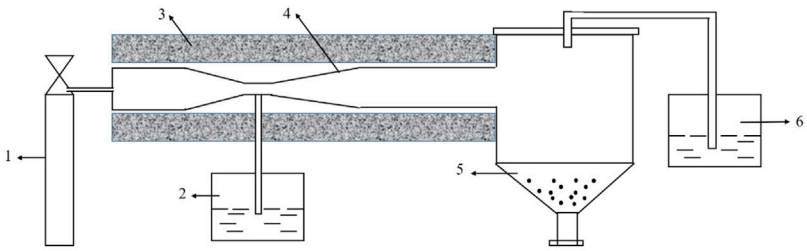

FIGURE 1 | Diagram of equipment. 1 oxygen bottle; 2 waste acid solution; 3 heating furnace; 4 Venturi reactor; 5 Solid product collector; 6 alkali liquor.

TABLE 1 | Pyrolysis conditions.

Condition	Value
Temperature (K)	773、873、923、973、1023、1123
$FeCl_2/FeCl_3$	1:0.5; 1:0.75; 1:1; 1:1.25; 1:1.5
$FeCl_2/C_6H_8O_7$	1:0.5; 1:1; 1:1.5; 1:2; 1:2.5

pyrolysis temperature and feed quantity. Moreover, computational fluid dynamics (CFD) was used to simulate the spray pressure and temperature distribution in a pyrolysis furnace. Lv et al. produced a mixture of gases and solids with the Venturi reactor, which improved the pyrolysis efficiency and prepared spherical $CeCl_3$ and Fe_2O_3 micro/nanoparticles (Lv et al., 2019a; Lv et al., 2019b; Lv et al., 2019c; Lv, 2019). Venturi reactor can enhance the mix of the gas and liquid, and solve the problem of Ruthner spray pyrolysis method that the nozzle needs to be replaced periodically. The simple structure and low investment of the Venturi reactor have resulted in its broad usage, but it is necessary to study it further. At present, there is a problem that the product particles are easy to accumulate and jam at the Venturi tube when the Venturi reactor is used for the pyrolysis reaction. Adding citric acid can well solve this problem. The carbon dioxide and water vapor are produced in the chemical reaction by citric acid. The gas-phase pressure can push the particles to flow to outlet, which prevents the jam at Venturi tube, increases the reaction efficiency and changes the morphology of the product particles.

This paper used a combination of experiments and numerical simulations to study the effects of temperature, pickling liquor composition, and citric acid ratio on the composition and morphology of Fe_2O_3 particles obtained at the outlet of a Venturi reactor. The effect on the Fe_2O_3 particle distribution in the reactor was also investigated. The results can be used to optimize the operating conditions of pyrolysis, as well as the pickling liquor, to provide a reference for the optimal design of Venturi reactors.

EXPERIMENTAL

Physical Experiments

A diagram of the equipment used in the jet pyrolysis experiments is shown in **Figure 1**. Oxygen was added by a high-speed air pump 1 into the Venturi reactor 4. The waste acid 2 mixed with citric acid, and then the mixed liquor dripped into the heating furnace 3. Pyrolysis occurred in the Venturi reactor 4. Next, the pyrolysis product Fe_2O_3 was collected by a particle collector, and tail gas was recovered by the alkali liquor in the recovery device 6. Venturi reactor is a place for evaporation, phase change and pyrolysis reaction. The reaction mechanism is not clear now, so the investigation of it should be focused on. Because of the mature separation technology of the gas and solid phase, we did not lay emphasis on it in this study. Employing the pyrolysis conditions summarized in **Table 1** and O_2, CO_2, HCl(g), H_2O(g), HCl(l), H_2O(l), $FeCl_2$, $FeCl_3$, and Fe_2O_3 as the chemical species involved in the reactions. Physical parameters of the substances were obtained from the handbook of practical inorganic thermodynamic data (Ye and Hu, 2002).

Numerical Simulations

According to the Venturi reactor dimensions, a geometric model with identical proportions was created in SolidWorks 2016, and ICEM 19.0 was used to divide the geometric model into a structured grid with a quantity of 410′000 (**Figure 2**).

Eulerian multiphase model, standard k-ε turbulence model and SIMPLE algorithm were selected in Fluent 19.0, the control equations were differentially treated using the second-order upwind scheme, and all items were converged to 10^{-4} except for energy (to 10^{-6}). The time step was set to 0.001 s, the computing time was 60 s and the simulation results were steady at the moment. The main reactions involved include:

$$H_2O(l) \rightarrow H_2O(g) \quad (1)$$

$$HCl(l) \rightarrow HCl(g) \quad (2)$$

$$2FeCl_2(s) + 2H_2O(g) + 1/2O_2(g) \rightarrow Fe_2O_3(s) + 4HCl(g) \quad (3)$$

$$2FeCl_3(s) + 3H_2O(g) \rightarrow 2Fe_2O_3(s) + 6HCl(g) \quad (4)$$

$$2C_6H_8O_7 + 9O_2(g) \rightarrow 12CO_2(s) + 8H_2O(g) \quad (5)$$

Besides the mass conservation equation, momentum conservation equation and energy conservation equation, it also involved the chemical reaction equation:

$$\frac{\partial(\rho Y_i)}{\partial t} + \nabla \cdot (\rho \overline{v} Y_i) = -\nabla \overline{J}_i + R_i + S_i \quad (6)$$

where Y_i is the mass fraction of the ith substance, R_i is the net produce rate of chemical reaction of the ith substance, S_i is the discrete phase of the ith substance and it is also the extra produce rate caused by the user-defined source item, J_i is the diffusive flux of the ith substance produced by the concentration gradient.

As shown in **Figure 2**, the section on the left side in the horizontal direction of the jet reactor was set as the O_2 inlet, the section on the

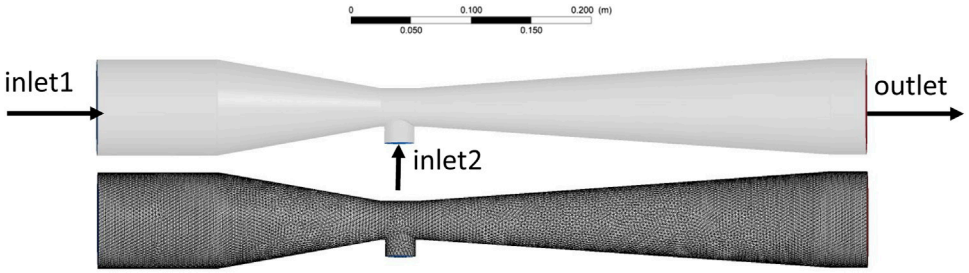

FIGURE 2 | Geometric models and mesh generation.

TABLE 2 | Boundary conditions.

	Inlet1-O_2	Inlet2-$FeCl_2$\$FeCl_3$	Outlet
Condition	Velocity-inlet	Velocity-inlet	Outflow
Value (m/s)	21.15	0.015 (10%$FeCl_2$, 5%-15%$FeCl_3$, 5%HCl, 0%-25%$C_6H_8O_7$)	—

TABLE 3 | Content comparison at outlet.

	Experimental result	Simulation results	Errors
Fe_2O_3(0%$C_6H_8O_7$)	2997.03 g/h	3211.24 g/h	6.67%
CO_2(0%$C_6H_8O_7$)	0 g/h	0 g/h	0%
Fe_2O_3(10%$C_6H_8O_7$)	3018.61 g/h	3289.25 g/h	8.23%
CO_2(10%$C_6H_8O_7$)	3382.76 g/h	3519.42 g/h	3.88%

right was the free outlet, and the section directly below the reactor in the vertical direction was the waste acid solution inlet.

Procedures

$FeCl_2$ and $FeCl_3$ solutions, each with a mass ratio of 10%, were prepared using deionized water, HCl, $FeCl_2$ and $FeCl_3$ solution ($FeCl_2$10% $FeCl_3$5%, $FeCl_2$10%$FeCl_3$7.5%, $FeCl_2$10%$FeCl_3$10%, $FeCl_2$10% $FeCl_3$12.5%, $FeCl_2$10%$FeCl_3$15%, the mass ratio of the two was 1:0.5, 1:0.75, 1:1, 1:1.25, and 1:1.5). Based on the prepared $FeCl_2$10%$FeCl_3$10% waste acid solution, a certain amount of citric acid was added to prepare a precursor solution with $FeCl_2$: $C_6H_8O_7$ mass ratios of 1:0.5, 1:1, 1:1.5, 1: 2, and 1:2.5. $FeCl_2$, $FeCl_3$, HCl, and $C_6H_8O_7$ were provided by Tianjin Fengchuan Chemical Reagent Technologies Co., Ltd. The real-time monitoring of the pyrolysis temperature was performed by the pyrolysis furnace. When the furnace reached the set temperature, the oxygen entered the Venturi reactor from the left inlet at a speed of 21.15 m/s under the carrier gas pressure, and the waste acid solution entered the Venturi reactor from the material inlet. The furnace temperature was set to 773, 873, 923, 973, 1023, and 1123 K, and the pyrolysis products Fe_2O_3 were collected at the cyclone separating unit.

RESULTS AND DISCUSSION

Verification of Simulation Result

The boundary conditions are shown in **Table 2**. The basic standard conditions of the research are 10%$FeCl_2$, 10%$FeCl_3$, 5%HCl, 0%$C_6H_8O_7$.

As shown in **Table 3**, the data results of Fe_2O_3 and CO_2 at outlet of the two representative conditions: adding no citric acid and adding 10% citric acid were compared. The errors between the experimental results of the collected Fe_2O_3 and CO_2 at the outlet and the numerical simulations was within 10%, which indicated the validity of the chosen model and the boundary conditions of the simulation. As shown in **Figure 3**, to further study the distribution of Fe_2O_3 in the reactor, five sections in the Venturi reactor were monitored.

Effects of Pyrolysis Temperature on the Pyrolysis Performance

The XRD phase analysis of products prepared under different pyrolysis temperatures was carried out from 10 to 80° at a scan rate of 7 °/min. As shown in **Figure 4**, the products prepared by jet pyrolysis under different temperatures all consisted of Fe_2O_3. Upon increasing the pyrolysis temperature, the intensity of the diffraction peak of (B-L) Fe_2O_3 first decreased and then gradually increased. The intensity of the diffraction peak of F −923 K was the smallest without an obvious peak of impurity phases, different crystal forms of Fe_2O_3 were possibly produced at 923 K.

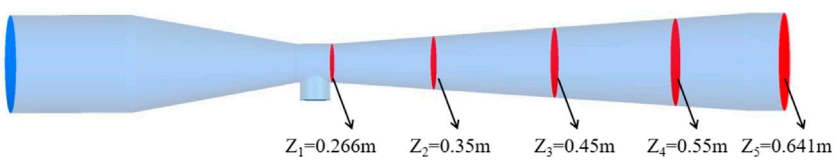

FIGURE 3 | Determination of monitoring surface.

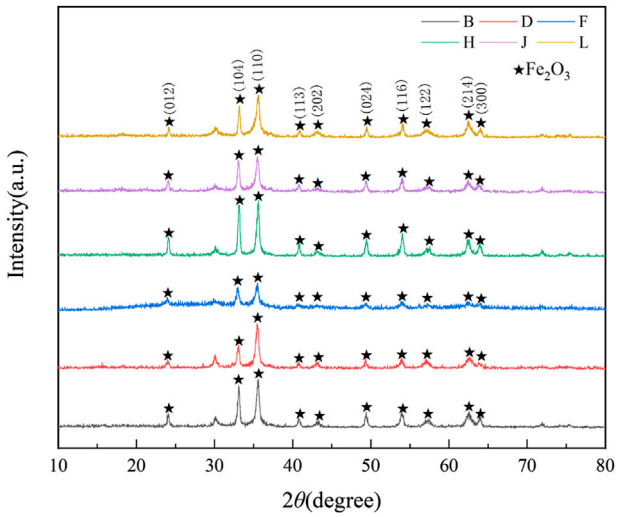

FIGURE 4 | XRD patterns of the pyrolysis products obtained at different temperatures. B-773, D-873K, F-923K, H-973K, J-1023K, L-1123K.

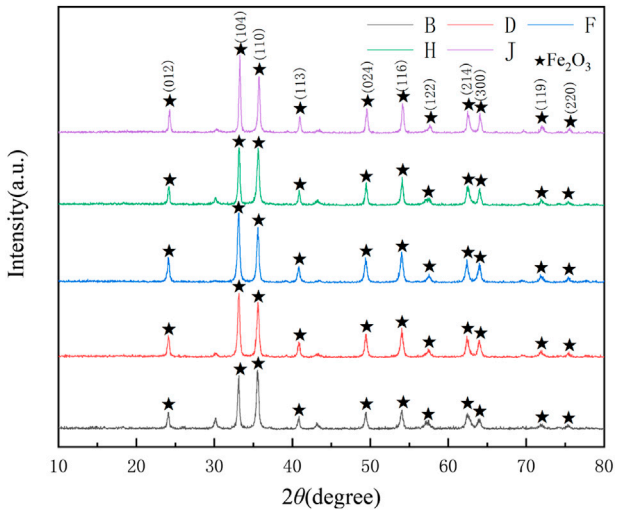

FIGURE 6 | XRD patterns of the pyrolysis products obtained at different $FeCl_2/FeCl_3$ ratios. B-1:0.5, D-1:0.75, F-1:1, H-1:1.25, J-1:1.5.

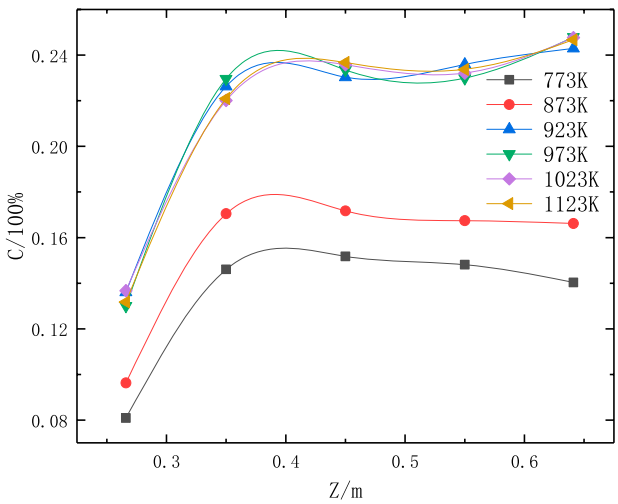

FIGURE 5 | The average Fe_2O_3 concentration on monitored surfaces at different temperatures.

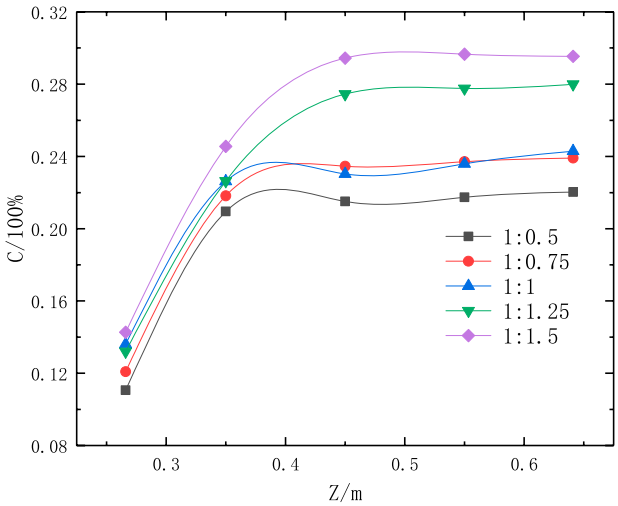

FIGURE 7 | Fe_2O_3 concentration on the monitored surfaces at different $FeCl_2/FeCl_3$ ratios.

According to the numerical simulation results (**Figure 5**), the average Fe_2O_3 concentration on various monitored surfaces in the reactor increased significantly upon increasing the pyrolysis temperature. When the pyrolysis temperature reached 923 K, further increasing the pyrolysis temperature did not affect the average concentration of Fe_2O_3 particles significantly. This indicates that 923 K is the optimal pyrolysis temperature.

Effects of Pickling Liquor Composition on Pyrolysis

When the pyrolysis temperature reached 923 K, the XRD phase analysis of products prepared using different $FeCl_2/FeCl_3$ ratios in the pickling liquor was conducted, and the results are shown in **Figure 6**. The products prepared by jet pyrolysis under different $FeCl_2/FeCl_3$ ratios all consisted of Fe_2O_3. The height of the crystal face 104 and 110 changed. As the $FeCl_2/FeCl_3$ ratio increased, (B-J) Fe_2O_3 grew along different crystal faces. When $FeCl_2$:$FeCl_3$ = 1:1, the Fe_2O_3 with the least impurities among all the cases was obtained, with the strongest diffraction peak intensity.

As shown in **Figure 7**, the Fe_2O_3 concentration in the reactor increased upon increasing the concentration of $FeCl_3$ in the pickling liquor. When $FeCl_2$:$FeCl_3$ = 1:1.5, the maximum average Fe_2O_3 particle concentration on various monitored surfaces in the reactor was obtained. This was because upon increasing the $FeCl_3$ concentration, the Fe ion content at the material inlet increased; thus, according to the

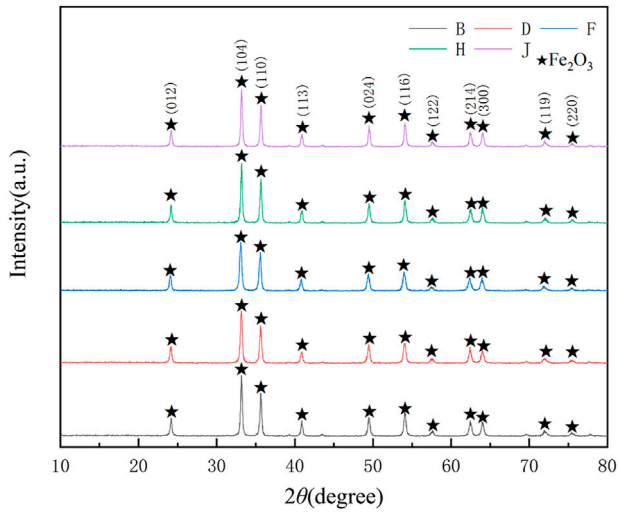

FIGURE 8 | XRD patterns of the pyrolysis products obtained using different citric acid ratios. B-1:0.5, D-1:1, F-1:1.5, H-1:2, J-1:2.5.

law of conservation, the concentration of Fe_2O_3 particles at the outlet also increased.

Effects of the Citric Acid Ratio During Pyrolysis

When the pyrolysis temperature reached 923 K, $FeCl_2$:$FeCl_3$ = 1:1, the XRD phase analysis of products prepared with different proportions of citric acid was carried out, and the results are shown in **Figure 8**. Adding citric acid contributed to a sufficient pyrolysis reaction and a disappearing of impurity peak. The products prepared by jet pyrolysis using different citric acid ratios all consisted of Fe_2O_3. Upon changing the pickling liquor ratio, there was no obvious change in the intensity of the diffraction peak of (B-J) Fe_2O_3, and the addition of more citric acid had no obvious effect on the product purity.

Figure 9 shows the SEM images of pyrolysis products using solutions with different citric acid ratios. As the citric acid ratio increased, the Fe_2O_3 particles aggregated and finally evolved into irregular sheets. This was because upon increasing the citric acid ratio, a great amount of gas was produced during the pyrolysis of citric acid under a high temperature, and the aggregated products exploded into fragments due to the gas pressure (Yang et al., 2017).

The integral area of each curve in **Figure 10** is shown in **Table 4**. When the concentration of the citric acid changed, increasing the citric acid ratio did not obviously affect the total amount of Fe_2O_3 particles in the reactor because the addition of citric acid did not change the total amount of Fe ions at the material inlet. The added citric acid changed the Fe_2O_3 particle distribution in the reactor—at a higher citric acid ratio, less Fe_2O_3 appeared on the first half of the monitored surface, and a higher Fe_2O_3 content appeared on the second half. This was because a large amount of gas (CO_2 and H_2O) was produced during the pyrolysis of citric acid. The flow of this gas changed the distribution of particle products in the Venturi reactor, which caused the particle product content to decrease in the first half of the reactor, while the particle product content increased in the second half.

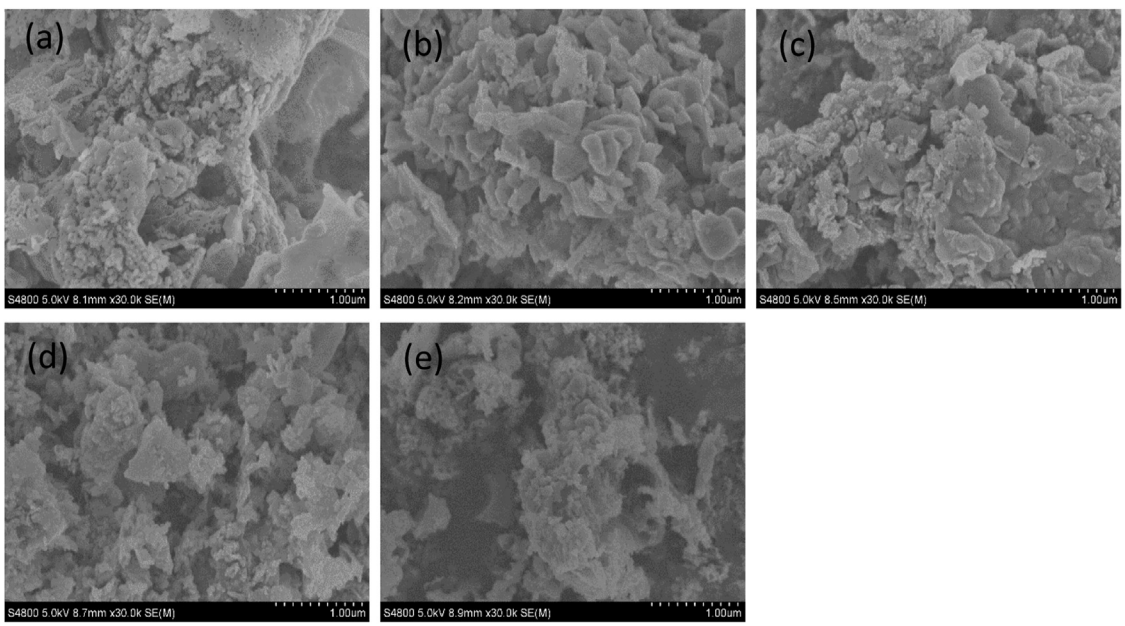

FIGURE 9 | SEM images of the pyrolysis products **(A)** 1:0.5 **(B)** 1:1 **(C)** 1:1.5 **(D)** 1:2 **(E)** 1:2.5.

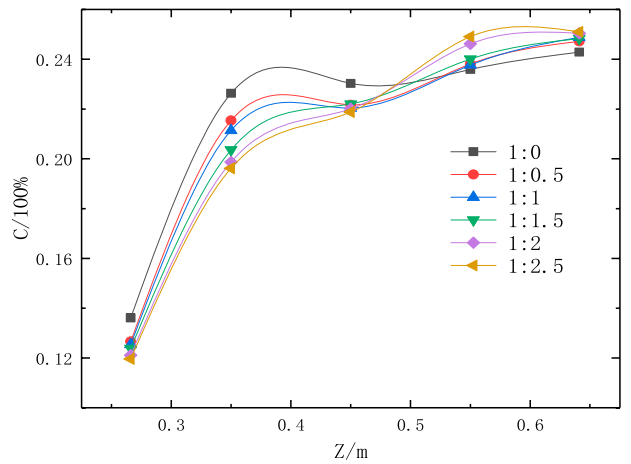

FIGURE 10 | Average Fe_2O_3 concentrations on monitored surfaces in the reactor at different citric acid ratios.

TABLE 4 | Integral areas of different curves.

Curve	1:0	1:0.5	1:1	1:1.5	1:2	1:2.5
Area	0.0813	0.0812	0.0810	0.0813	0.0812	0.0811

CONCLUSION

As the pyrolysis temperature increased, the concentration of Fe_2O_3 particles in the reactor increased. At 923 K, the purity and concentration of Fe_2O_3 were maximized, and further increasing the pyrolysis temperature had negligible effects on the concentration of Fe_2O_3 particles at the outlet. When FeCl2:FeCl3 = 1:1, the Fe2O3 with the least impurities among all the cases was obtained. When $FeCl_2$/$FeCl_3$ = 1:1.5, the concentration of Fe_2O_3 particles at the outlet was maximized. The ratio of citric acid possibly changed size distribution of Fe_2O_3 particles and their distribution in the reactor. When the ratio of $FeCl_2/C_6H_8O_7$ was1:1, the size distribution of Fe_2O_3 particles was homogeneous, and when the ratio of $FeCl_2/C_6H_8O_7$ was1: 2.5, the concentration of Fe_2O_3 particles at the outlet was maximized.

DATA AVAILABILITY STATEMENT

The raw data supporting the conclusion of this article will be made available by the authors, without undue reservation.

AUTHOR CONTRIBUTIONS

CL: Conceptualization, Funding acquisition, Project administration; M-HS: Data curation, Writing—original, draft; H-XY: Software.

FUNDING

This research was supported by the National Natural Science Foundation of China (51904069), the open fund of the Key Laboratory of iron and steel metallurgy and resource utilization of Wuhan University of science and technology (FMRU19-1), the Scientific Research Fund project of Northeastern University at Qinhuangdao (XNY201808), the Natural Science Foundation of Hebei Province of China (E2019501085).

REFERENCES

Bian, X., Wang, Z. F., Wang, J. Y., and Wu, W. (2015). Preparation of Lanthanum Hydroxide by Spray Pyrolysis of Lanthanum Chloride. *J. Northeast. Univ. (Natural Science)* 7, 966–969. doi:10.3969/j.issn.1005-3026.2015.07.012

Deng, X. R., Hu, G. R., Peng, Z. D., and Yoon, S. G. (2007). Spherical (Y, Gd) BO3: Eu Phosphor Particles Prepared by Spray Pyrolysis. *J. Chin. Rare Earth Soc.* 2, 167–171. doi:10.3969/j.issn.1000-4343.2007.02.0167.05

Fang, Z. Q., Qiu, X. H., Chen, J. H., Kim, E. J., and Chang, Y. S. (2010). Degradation of the Polybrominated Diphenyl Ethers by Nanoscale Zero-Valent Metallic Particles Prepared from Steel Pickling Waste Liquor. *Desalination* 1, 34–41. doi:10.1016/j.desal.2010.09.003

Gao, J.-m., Du, Z., Ma, S., Cheng, F., and Li, P. (2021). High-efficiency Leaching of Valuable Metals from Saprolite Laterite Ore Using Pickling Waste Liquor for Synthesis of Spinel-type Ferrites MFe2O4 with Excellent Magnetic Properties. *J. Mater. Res. Tech.* 10, 988–1001. doi:10.1016/j.jmrt.2020.12.063

Izumi, T., Norifumi, F., and Muxina, K. (2007). Synthesis of Spherical LiMn2O4 Microparticles by a Combination of spray Pyrolysis and Drying Method. *Powder Tech.* 3, 228–236. doi:10.1016/j.powtec.2007.05.011

Liu, Y. T., Liu, F. Z., and Du, W. (2018). Preparation of Magnesium Oxide from Bischofite by Spray Pyrolysis. *J. Mater. Sci. Eng.* 6, 1010–1015. doi:10.14136/j.cnki.issn1673-2812.2018.06.028

Lv, C. (2019). Numerical Simulation on the Recovery Process of Acid Pickling Waste Liquor by Jet-Flow Pyrolysis. *JOM* 71, 4944–4949. doi:10.1007/s11837-019-03827-8

Lv, C., Zhang, T.-A., Dou, Z.-H., and Zhao, Q.-Y. (2019a). Numerical Simulation of Preparation of Ultrafine Cerium Oxides Using Jet-Flow Pyrolysis. *Rare Met.* 38, 1160–1168. doi:10.1007/s12598-019-01337-9

Lv, C., Zhang, T. A., Dou, Z., and Zhao, Q. (2019b). Simulation of Process and Reactor Structure Optimization for CeO2 Preparation from Jet-Flow Pyrolysis. *JOM* 71, 1660–1666. doi:10.1007/s11837-019-03397-9

Lv, C., Zhang, T. A., and Hao, B. (2019c). Simulation of the Scale-Up Process of a Venturi Jet Pyrolysis Reactor. *Metals* 9, 979–987. doi:10.3390/met9090979

Qi, F. X. (2006). *Research on Rare Earth Dopted Yttrium Aluminum Garnet Phosphor Synthesized by Spray Pyrolysis*. Nanjing: Nanjing University of Eechnology. [dissertation/master's thesis].

Sun, T. H., Hao, S. J., Jiang, W. F., and Zhang, Y. Z. (2021). Preparation and Morphology Analysis of Nano-Sized Iron Oxide. *Powder Metall. Tech.* 1, 76–80. doi:10.19591/j.cnki.cn11-1974/tf.2019080008

Wang, J. G., and Ma, Q. (2017). Harmless Disposal and Resource Utilization of Pickling Waste Liquid from Iron and Steel Plant. *Shandong Chem. Industry* 21, 184–185. doi:10.19319/j.cnki.issn.1008-021x.2017.21.075

Wang, S. S., Huang, S. W., and Lu, Y. C. (2020). Analysis and Research on Hydrochloric Acid Pickling Waste Liquid in Iron and Steel Plant. *J. Beibu Gulf Univ.* 2, 25–28. doi:10.19703/j.bbgu.2096-7276.2020.02.0025

Yang, G. S., Bian, X., and Cui, L. X. (2017). Study on Preparation of Nano Cerium Oxide Powder by Spray Roasting of Cerium Chloride Solution. *Chin. Rare Earths* 1, 72–78. doi:10.16533/J.CNKI.15-1099/TF.201701013

Ye, D. L., and Hu, J. H. (2002). *Handbook of Practical Inorganic Thermodynamic Data*. Beijing: Metallurgical industry press.

Zhang, R. Z., Hu, Q. H., Pei, Y. W., and Song, X. (2014). Resources Utilization of Hydrochloric Pickling Waste Liquor by Technology of Salt-Added Distillation and Coagulant Preparation. *Chin. J. Environ. Eng.* 11, 4782–4787. doi:10.7513/j.issn.1004-7638.2020.03.020

Zhang, Y., Lin, L., and Zhu, X. J. (2020). Preparation of α-nanometer Iron Oxide by Microwave Hydrolysis. *Iron Steel Vanadium Titanium* 3, 116–121. doi:10.3969/j.issn.1673-9108.2014.11.4782.06

Conflict of Interest: The authors declare that the research was conducted in the absence of any commercial or financial relationships that could be construed as a potential conflict of interest.

Publisher's Note: All claims expressed in this article are solely those of the authors and do not necessarily represent those of their affiliated organizations, or those of the publisher, the editors and the reviewers. Any product that may be evaluated in this article, or claim that may be made by its manufacturer, is not guaranteed or endorsed by the publisher.

Copyright © 2021 Lv, Sun and Yin. This is an open-access article distributed under the terms of the Creative Commons Attribution License (CC BY). The use, distribution or reproduction in other forums is permitted, provided the original author(s) and the copyright owner(s) are credited and that the original publication in this journal is cited, in accordance with accepted academic practice. No use, distribution or reproduction is permitted which does not comply with these terms.